Ionochromic Effects and Structures of Metalated Poly(*p*-phenylenevinylene) Polymers Incorporating 2,2′-Bipyridines

Lin X. Chen,*,† Wighard J. H. Jäger,† David J. Gosztola,† Mark P. Niemczyk,† and Michael R. Wasielewski*,†,‡

Chemistry Division, Argonne National Laboratory, Argonne, Illinois 60439, and Department of Chemistry, Northwestern University, Evanston, Illinois 60208-3113

Received: September 21, 1999; In Final Form: December 20, 1999

The effects of metal ion chelation to the 2,2′-bipyridine (bpy) groups on the photophysics and exciton dynamics of two conjugated polymers **1** and **2** in solution are investigated. The structures of polymers **1** and **2** have 2,2′-bipyridyl-5-vinylene units that alternate with one and three 2,5-bis(*n*-decyloxy)-1,4-phenylenevinylene monomer units, respectively. The photophysics and exciton dynamics of metalated polymers **1** and **2** are compared to those of the metal-free polymers (Chen et al. *J. Phys. Chem. A* **1999**, *103*, 4341−4351). The origins of ionochromic effects due the metal ion chelation were studied using both steady-state and transient optical spectroscopy, and the results indicate that both conformational flattening and participation of π electrons from the metal in the π-conjugation of the polymer backbone play important roles in metal ion binding induced red shifts in absorption and photoluminescence spectra. The photoluminescence properties of the metalated polymers are determined by the metal ion electronic structures, where the closed shell Zn^{2+}-bound polymer **2** has an increased photoluminescence quantum yield and the corresponding open shell Ni^{2+}- or Fe^{3+}-bound polymers have quenched photoluminescence due to spin−orbit coupling. The dual character of metalated polymer **2** as a conjugated polymer and as a metal−bpy complex is discussed. In addition, the structures of metal ion binding sites are studied via X-ray absorption fine structure (XAFS) and are related to the photophysical properties of the metalated polymers.

Introduction

The importance of π-conjugated polymers as optical materials has been well-recognized and extensively studied. One of the most commonly used organic optical materials is poly(phenylenevinylene) (PPV) and its derivatives.[1−7] Extensive efforts have been made to vary properties of PPV by attaching different functional groups in the backbone or in the side chains and by doping PPV with different small molecules or metal ions. Several conjugated polymers have been developed for applications, such as photorefractive materials,[8] metal ion sensing,[9−11] and molecular wires.[12−14] During recent years, 2,2′-bipyridine (bpy) has been incorporated into conjugated polymer backbones where metal−bpy complexes are formed.[8−10,15−17] The formation of metal−bpy complexes drastically alters the electronic structures, and consequently, the optical properties of the polymers. In a previous study, two bpy-containing PPV derivatives, polymers **1** and **2** (Figure 1), were synthesized, which incorporated one bpy unit for every one and three phenylenevinylene (PV) units.[9] Different metal ions can be chelated by the bpy units along the polymer backbone, resulting in metal ion specific ionochromic effects in absorption and emission spectra.[9,18] Two possible metal−bpy binding structures were suggested:[9] (1) bidentate chelation with both 2,2′ N atoms of a bpy group, which restores π-conjugation by restricting rotations along the C−C bond connecting two pyridyl rings, and (2) monodentate chelation with one of the N atoms in a bpy group, which may hinder a planar conformation along the polymer backbone.

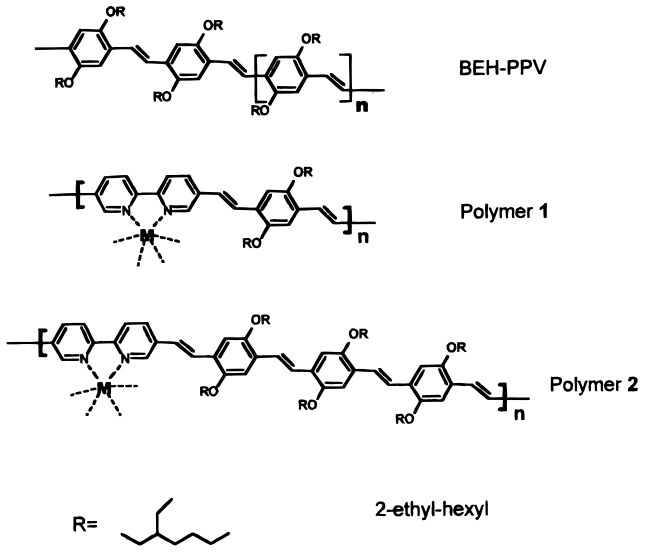

Figure 1. Molecular structures of polymers.

Our recent study systematically investigated the optical properties of polymers **1** and **2** as well as those of BEH−PPV (poly(2,5-bis-2′-ethylhexyloxyphenylenevinylene)), a well-conjugated PPV derivative, showing that bpy groups incorporated along the polymer backbone cause a series of changes in the optical properties of the polymers.[18] These changes can be explained by π-conjugation attenuation along the polymer backbone due to nonplanar conformations along the polymer

* To whom correspondence should be addressed.
† Argonne National Laboratory.
‡ Northwestern University.

10.1021/jp993365i CCC: $19.00
Published on Web 02/04/2000

backbone caused by rotations along the C−C bond connecting the two pyridine rings in the bpy groups, and a reduction of electronic interactions between PV and adjacent bpy groups because of their electronic structural differences. In this study, the optical properties, in particular the ionochromic effects, of metal-ion-incorporated polymers **1** and **2** are investigated. Structural studies on metal ion binding sites of the polymers using X-ray absorption fine structure (XAFS) are carried out to verify previously suggested different metal ion chelation structures. In addition, photophysics and exciton dynamics for metal-ion-incorporated polymers are examined with steady-state and transient optical spectroscopy. Finally, the optical properties and the structures of the metal ion binding sites are combined to establish structure/function relationships for the metal ion binding polymers and their potential applications in photonics.

Experimental Section

Synthesis of Polymer 1 and Polymer 2 and Metal−bpy Complexes. The synthesis of the polymers follows the procedures in previous studies.[9] Molecular weights for BEH−PPV, polymers **1** and **2**, are 200k, 6.4k, and 22k, respectively. The polymers were dissolved in toluene (Aldrich) at concentrations around 1×10^{-5} M.

The syntheses of simple metal−bpy complexes follow procedures from the literature.[19] In all cases, the bpy:M^{2+} ratio is ≥ 3 for $M^{2+} = Zn^{2+}$, Ni^{2+}, and Cu^{2+} and is ≥ 2 for $M^{2+} = Pd^{2+}$. The bpy complexes were recrystallized and their spectra agree with the literature values. $[Fe^{II}(bpy)_3]PF_6$ and $[Fe^{III}(bpy)_3]$-PF_6 complexes were purchased from Aldrich and were used without purification.

Metal Ion Titration. Each metal ion titration experiment was started with a 4.0 mL polymer toluene solution with a known concentration (about 10^{-5} M) of the monomer. The concentration was determined by the optical density at 439 nm for polymer **1** and at 469 nm for polymer **2**, respectively. Solutions (1 mM) of metal salt (acetate or sulfate) in methanol were used for the titration. A 1 μL aliquot of the salt solution was added each time to the polymer solution. The solution was stirred constantly during the titration. Steady-state optical absorption spectra were monitored 5 min after each addition of the metal ion using a Shimadzu UV−visible spectrophotometer (UV-1601). For the Pd^{2+} titration, binding reached equilibrium over 1 h after each addition of the Pd^{2+} solution.

Photoluminescence Spectra and Lifetime Measurements. The fluorescence spectra were taken with a fluorometer (Fluorescence Master Series) from Photon Technology International. A 1 cm path cuvette was used, and the fluorescence was collected at a right angle with respect to the incident light. Polymer solutions with $\sim 10^{-6}$ M concentration were used for the measurements.

Fluorescence lifetimes of the polymer solutions were measured by a time-correlated single photon counting (TCSPC) apparatus.[20] The samples were excited by 402 nm light pulses from a mode-locked, cavity-dumped, frequency-doubled Ti: sapphire laser system. The fluorescence signals were collected at a right angle with respect to the excitation laser beam through a lens and a monochromator with a 2 nm band-pass. A Hamamatsu microchannel plate detector (model R3809U-51) was used in conjunction with a Pico Timing system from EG&G ORTEC. A signal from a photodiode detecting a fraction of the excitation laser pulse was used as the "start" signal of the time-to-amplitude converter after being processed by a constant fraction discriminator (CFD, EG & G 9308). The fluorescence signal was used as the "stop" signal after being processed by another CFD. The instrument response function was taken using a dilute nondairy creamer suspension. The width of the instrument response function is about 50 ps (fwhm).

Transient Absorption Spectroscopy. The transient absorption setup with a Ti:sapphire regenerative amplifier and an optical parametric amplifier (OPA) has been described elsewhere.[21] The setup used for the experiments described here is identical to that for the studies of metal-free polymer solutions in our previous paper.[18] The excitation pulses were obtained from either the second harmonic of the output from the Ti:sapphire regenerative amplifier at 417 nm or from an optical parametric amplifier (OPA) at a selected wavelength. The probe pulses were obtained from the white light generated by focusing a fraction of the output from the regenerative amplifier to a sapphire window. The probe beam was split into two beams with one passing through the sample, while the other served as a reference beam. One of the probe beams was coincident with the pump beam. The optical density of the sample at the pump wavelength was kept below 0.3. The energy of the pump pulse was about 0.3 μJ, and the pump beam and white light were focused at the sample cuvette into $\sim$0.3 mm spots. The instrument response time was $\sim$180 fs.

Stock solutions of polymers were freshly made and the solution samples were checked periodically by a UV−visible spectrometer during laser experiments for possible photodegradation. The solutions were stirred and refreshed every 10 min from the stock solutions, judging by their optical absorption spectra. All spectroscopic studies were performed at room temperature.

XAFS Measurements. For the XAFS studies, most samples were polymer films. The films were made by drying chloroform solutions of the polymers on Mylar film substrates under a nitrogen atmosphere. The metal chelation for each film sample was carried out in solution with slightly lower than 1:1 stoichiometry of the bpy sites to the metal ions to ensure that no extra metal ions were present. The XAFS spectra were collected via X-ray fluorescence detection using a Lytle detector. For the Pd K-edge, Kr gas was used inside the detector chamber. For Ni, Cu, Fe, and Zn K-edges, Ar gas was used. Of all the measurements, X-ray transmission signals were collected simultaneously. The third ion chamber detector was setup to collect a reference transmission spectrum of the metal foil corresponding to the metal doped in the polymer films. Most of the XAFS experiments were conducted at Beamline X18B and X19A at NSLS (National Synchrotron Light Source, Brookhaven National Laboratory) and the Pd K-edge XAFS spectra for the $[Pd(bpy)_2]Cl_2$ and Pd^{2+}−polymer **1** solution were collected at Beamline 12BM, APS (Advanced Photon Source at Argonne National Laboratory). Si 111 crystals were used in the monochromators at the beamlines of NSLS with 60−70% detuning. An additional mirror was used in 12BM at APS for rejecting higher harmonics of the X-rays. The X-ray beam sizes at the samples were 1.5 cm horizontal and 0.1 cm vertical at X18B and 12BM and 0.05 cm vertical and 0.1 cm horizontal at X19A. Standard XAFS analysis programs were used in the data analysis. Fourier transforms of the XAFS spectra were taken between $k = 2.5$ and 12 A^{-1} for most of the samples and k^3 weighting was used.

Results

Optical Absorption Spectra and Metal Ion Titration. Ionochromic effects in the optical absorption spectra of metalated polymer solutions were observed in a previous study[9] and illustrated in Figure 2. Several spectral characteristics are

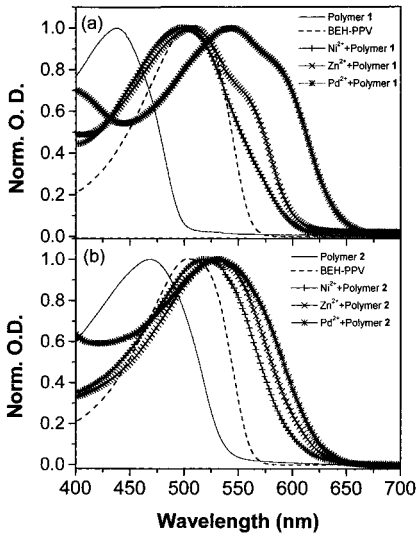

Figure 2. Optical absorption spectra of metalated polymers.

depicted: (1) metal ion binding causes red shifts in the absorption peaks relative to those in the metal-free polymers, (2) red-shifted absorption peaks are at lower energies than those in BEH−PPV, (3) the magnitude of the red shifts in polymer **1** are greater than those in polymer **2**, and (4) the red shifts are metal specific, the ionochromic effect. In addition, the absorption peaks of metalated polymer **1** have shoulders at the red sides that are not present in polymer **2**.

To investigate the origins of the ionochromic effects, a correlation between spectral shifts and metal ion concentration needs to be established. On the basis of previous studies,[18] conjugated polymers in solution can be viewed as an ensemble of segments of different conjugation lengths, which are responsible for their broad optical absorption peaks. The lower energy side of the absorption peak results from longer conjugated segments, while the higher energy side results from shorter conjugated segments. When metal ions are chelated to the bpy sites, the lengths of conjugated segments are changed, which can be monitored through the absorption spectra of polymers in solution as a function of metal ion concentration, from which the stoichiometry of metal ion binding and the origins of ionochromic effect may be obtained.

Metal ion titration curves are presented in Figure 3. On the left side of each figure, the absorption spectra are recorded as a function of metal ion concentration. On the right side, the optical densities (OD) at two or three characteristic wavelengths are displayed as functions of the concentration of the metal ions. These particular wavelengths were chosen because they represent the disappearance of the absorption peak of the metal-free polymer spectra and the appearance of the absorption peak in metalated polymer spectra. There are clearly several differences between the two sets of the spectra.

For polymer **1**, the isosbestic point in each of the titration curves is not well-defined. The optical density (OD) vs metal ion concentration plots monitored at the peak positions of the initial metal-free polymer solution and the final ∼100% metalated polymer solution are poorly correlated. This is an indication that more than two species with characteristic absorption spectra were present during the titration. Moreover, multiple peaks appear in the 100% metalated polymer absorption spectra, especially for Zn^{2+}- and Pd^{2+}-bound polymers. In contrast, isosbestic points for the titration curves of polymer **2** are rather well-defined, and the OD vs metal ion concentration curves monitored at the initial and final peak positions are correlated, implying the presence of two species with characteristic absorption spectra. Each of the final metal-bound polymer solutions still has a single absorption peak, rather than a shoulder on the red side of the main peak. Titration of the same metal ions into BEH−PPV solutions (not shown) did not result in any red shift of the spectra, indicating that the red shifts are indeed due to the metal ion binding. The titration results also reveal that metal ion binding to polymers **1** and **2** is not only controlled thermodynamically but also kinetically. For example, 1−2 h is required to complete the red shift of the absorption peak following each addition of Pd^{2+} to the polymer solutions, whereas only a few minutes are required for other metal ions. The gap in the Pd^{2+} to polymer **1** titration curve reflects the absorption change after a 1.5 h period. The Pd^{2+} titration in polymer **2** was incomplete after a 10 h period. Although, Pd^{2+} complexes of these polymers produce the largest red shifts among all the metal ions tested, complex formation appears to be kinetically least favorable.

Because isosbestic points of metal ion titration curves in polymer **2** are well-defined, binding constant K_b for the metal ions may be estimated, assuming that only two absorbing species, polymer **2** and the metalated polymer **2**, are present. Thus, the OD in Figure 3b can be expressed as

$$\mathrm{OD} = f_{\mathrm{MbpyP}}\mathrm{OD}_{\mathrm{MbpyP}} + f_{\mathrm{bpyP}}\mathrm{OD}_{\mathrm{bpyP}} \qquad (1)$$

where M, MbpyP, and bpyP designate metal ions, metalated polymer, and metal-free polymer, respectively. f is the fraction of the species. Equation 1 assumes that the following three factors are negligible: (a) the absorption from free metal ions in the solvent, (b) multiple bpy bindings to the same metal ion, and (c) the influence between the neighboring metal ion binding sites. Using the spectra of the metal-free polymer and the 100% metalated polymer as references denoted by OD(0) and OD(M), the concentrations of MbpyP and remaining bpyP can be estimated by

$$[\mathrm{bpyP}] = f_{\mathrm{bpyP}}[\mathrm{bpyP}]_0 = \frac{\mathrm{OD} - \mathrm{OD(M)}}{\mathrm{OD(0)} - \mathrm{OD(M)}}[\mathrm{bpyP}]_0$$

$$[\mathrm{MbpyP}] = f_{\mathrm{MbpyP}}[\mathrm{bpyP}]_0 = \frac{\mathrm{OD} - \mathrm{OD(0)}}{\mathrm{OD(M)} - \mathrm{OD(0)}}[\mathrm{bpyP}]_0$$

$$[\mathrm{M}] = [\mathrm{M}]_0 - [\mathrm{MbpyP}] \qquad (2)$$

where $[M]_0$ and $[bpyP]_0$ are initial concentrations for the metal ions and the bpy groups in polymer chains, respectively. In addition, because the two-state model describes the absorption change during the titration, the binding of a particular bpy site is independent of the occupancy of the neighboring site. Therefore, the binding constant for metal ions in polymer **2** can be calculated as the following:

$$K_b = \frac{[\mathrm{MbpyP}]}{[\mathrm{M}][\mathrm{bpyP}]} \qquad (3)$$

K_b for Fe^{2+}, Zn^{2+}, and Ni^{2+} are estimated to be 1×10^5, 3×10^5, and 4×10^5 M^{-1}, respectively.

Photoluminescence Spectra of Polymer 2 Chelated by Zn^{2+} and Ni^{2+}. Effects of the metal ion binding on the photoluminescence (PL) properties of the polymers **1** and **2** may have important applications in photonics. These effects were first investigated by steady-state photoluminescence. Polymer **2** complexes with Zn^{2+} and Ni^{2+} were studied, where the former has a closed shell d^{10} configuration and the latter, an open shell d^8 configuration. Figure 4a depicts steady-state PL spectra of

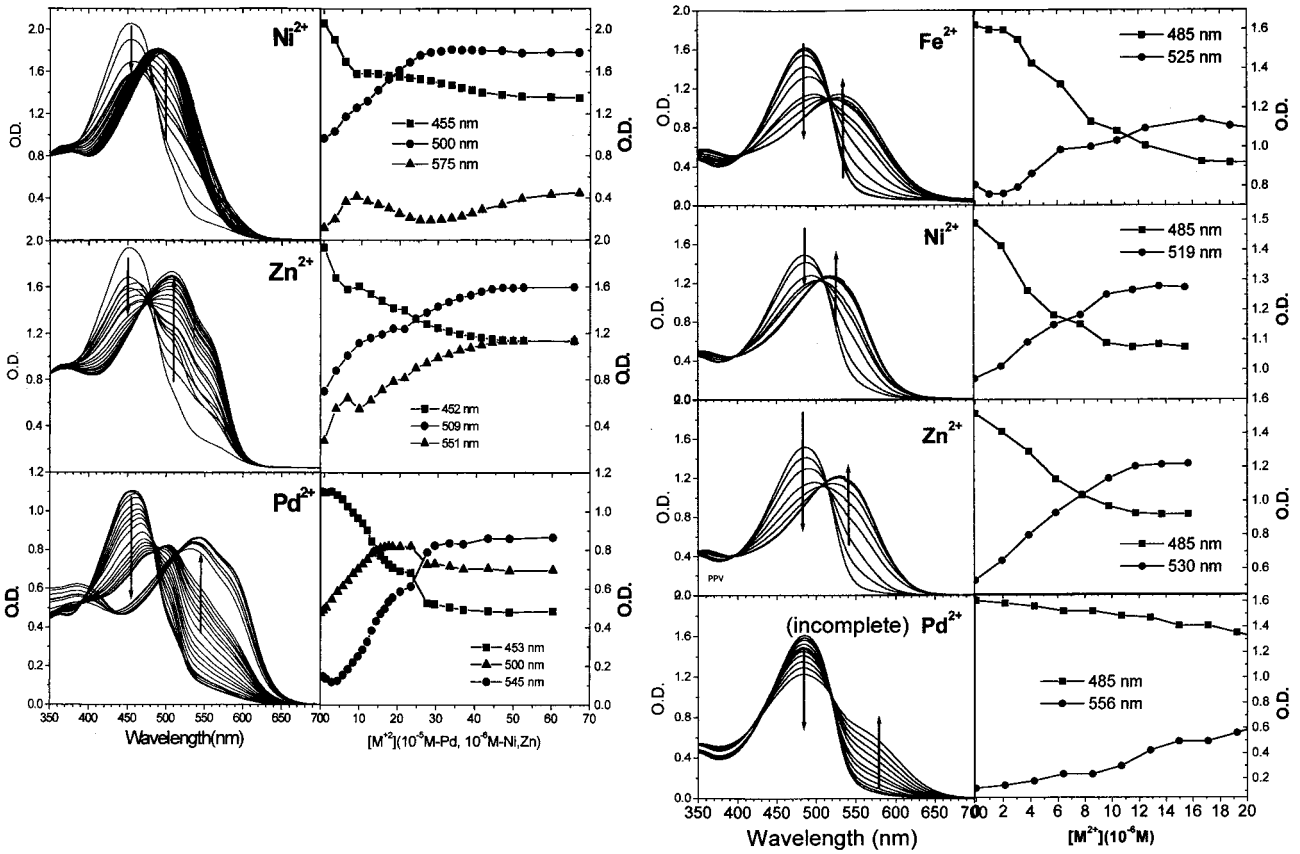

Figure 3. Titration curves of polymers (a) polymer **1** and (b) polymer **2**. The left panels are the optical absorption spectra of the polymer as a function of the metal ion concentration; the arrows indicate the direction of the change as metal ions were added. The right panels are the optical densities at a few characteristic wavelengths as a function of the metal ion concentration.

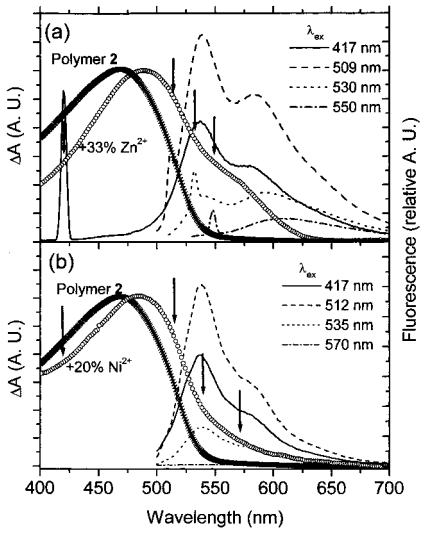

Figure 4. Steady-state photoluminescence of partially occupied Zn^{2+} (a) and Ni^{2+} polymer **2** complexes. The arrows indicated the excitation wavelengths. The spectra are not corrected for the wavelength dependence of the fluorometer.

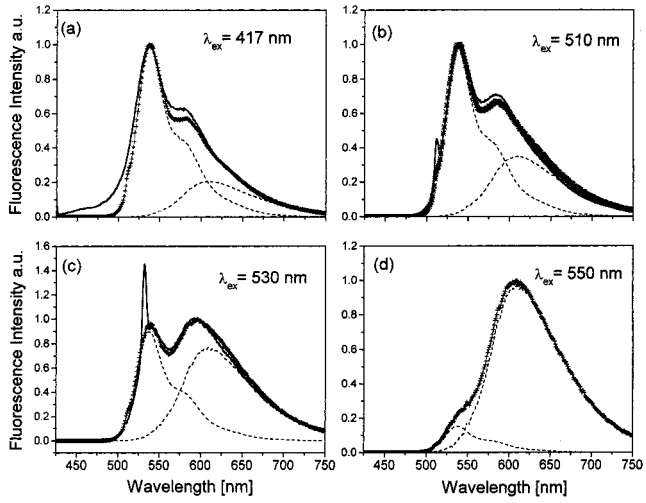

Figure 5. Photoluminescence of 25% Zn^{2+}-occupied polymer **2** as a function of excitation wavelength. The solid is observed the spectra. The +++ lines are reconstructed spectra from PL spectra of neat and 100% Zn^{2+}-occupied polymer **2** (dashed lines: on the left, the metal-free polymer; on the right, 100% Zn^{2+}-occupied polymer).

33% Zn^{2+}-bound polymer **2** at different excitation wavelengths λ_{ex}. In contrast to previously observed PL spectra for the metal-free polymers **1** and **2**,[18] where little λ_{ex} dependence was observed, 33% Zn^{2+}-bound polymer **2** shows a strong λ_{ex} dependence in its PL spectrum. As λ_{ex} becomes longer, the intensity of the absorption peak at 540 nm, corresponding to the 0−0 transition in the metal-free polymer **2**, becomes weaker relative to a shoulder on the red side of the peak around 590 nm. At $\lambda_{ex} \approx 550$ nm where metal-free polymer **2** has very little absorption, the PL spectrum is dominated by a broad peak with a maximum around 615 nm, which resembles the PL spectrum of 100% Zn^{2+}-bound polymer **2**. Figure 5 displays the observed PL spectra of a 33% Zn^{2+}-bound polymer **2** with different λ_{ex} and those reconstructed from PL spectra of neat and 100% Zn^{2+}-bound polymer **2**. The reconstructed PL spectra agree well with the observed spectra, confirming that a two-state model is appropriate for describing the PL spectra of partially Zn^{2+}-occupied polymer **2**, as we have seen in the

absorption spectra from the metal ion titration. As λ_{ex} gets longer, the fraction of the PL from metal-free polymer **2** in the reconstructed spectra gets smaller, while that from Zn^{2+}-bound polymer **2** becomes more dominant. Unlike the metal-free polymers in which the emission always comes from the same origin independent of λ_{ex}, partially Zn^{2+}-bound polymer **2** has two distinguishable emitting species that can be preferentially excited by different λ_{ex}. Although the absorption and the emission of the Zn^{2+}-bound segments of the polymer have lower energies compared to their counterpart of the metal-free polymer, the PL originated from the metal-free polymer segments was not quenched due to the energy flow to the Zn^{2+}-occupied segments. The two chemically different species emit independently with little interaction between each other. This quantum confinement is likely from incompatibility in electronic structures between Zn^{2+}-bound and metal-free sections of polymer **2**, which results in barriers for exciton diffusion along the chain as we have discussed in our previous studies.[18] The relative PL quantum yield of Zn^{2+}-bound polymer **2** to that of the metal-free polymer can be estimated from the absorption and luminescence spectra of neat, 100% and 33% Zn^{2+}-doped polymer **2**. The estimated relative luminescence quantum yield of 100% Zn^{2+}-bound polymer **2** is about 1.7−2.0 times of that of the metal-free polymer **2**.

PL for 20% Ni^{2+}-bound polymer **2** appears very differently from its Zn^{2+} counterpart. Figure 4b depicts the PL of 20% Ni^{2+}-bound polymer **2** excited at different λ_{ex}. Instead of showing the spectral shape variation as in Zn^{2+} case (see Figures 4a and 5), the shape of the PL spectra is largely independent of λ_{ex}. When λ_{ex} is lower in energy than the red edge of the absorption spectrum of the metal-free polymer **2**, but is still higher in energy than Ni^{2+}-bound polymer absorption (e.g., $\lambda_{ex} = 570$ nm), there is no measurable PL. This indicates that the excited states of Ni^{2+}−bpy complex segments in polymer **2** undergo a nonradiative decay process, similar to the $[Ni(bpy)_3]^{2+}$ complex. Because the open shell electronic structure of Ni^{2+} involves strong spin−orbit coupling between the metal and the ligand, the PL is quenched. The fact that Ni^{2+}-bound polymer luminescence is linearly proportional to the remaining portions of the metal-free polymer, again suggests weak interactions between the metal-bound and metal-free segments of the polymer.

Photodynamics of Metalated Polymers. Although the steady-state PL spectra of the metalated polymers indicate that the metalated and the metal-free segments of the polymer do not interact strongly, energy and electron-transfer processes between the segments may occur within a very short time after the photoexcitation. Therefore, fast photodynamics studies are useful in revealing such processes.

As was observed for the metal-free polymer **2** solution in the previous study,[18] transient absorption spectra of metalated polymer **2** in solution appear to have ground-state bleaching, stimulated emission, and photoinduced absorption regions. Unfortunately, the absorption and emission spectra for metalated polymer **2** are red-shifted, so the stimulated emission region overlaps with the photoinduced absorption region shown in Figure 6b,c. For 25% and 100% Zn^{2+}-bound polymer **2**, the early time transient absorption spectra (Figure 6b,c) are distinctively different from that of metal-free polymer **2** (Figure 6a). The original stimulated emission region for metal-free polymer **2** between 520 and 600 nm now consists of a superposition of the stimulated emission from metal-free segments and the ground-state bleaching of Zn^{2+}-bound segments peaked around 520 nm and the photoinduced absorption that

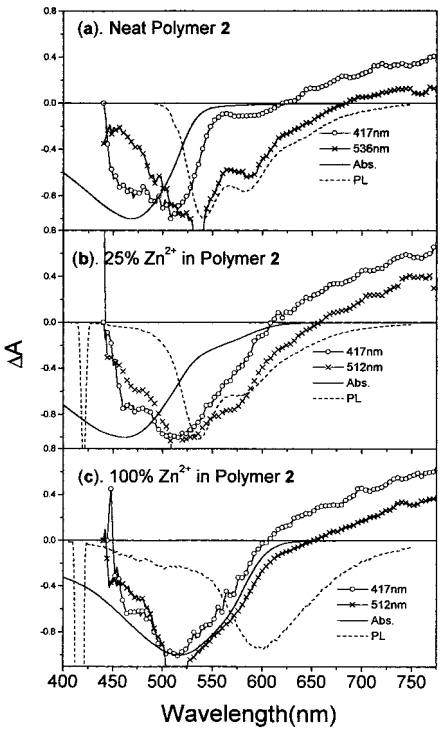

Figure 6. Transient absorption spectra at 1 ps after excitation for (a) polymer **2**, (b) 25%-occupied Zn^{2+} polymer **2**, and (c) 100% Zn^{2+}-occupied polymer **2** along with their absorption and PL spectra.

TABLE 1: Photoinduced Absorption Kinetics of Polymer 2 with Metal Ions (Monitored at 740 nm)

sample	A_1 (%)	τ_1 (ps)	A_2 (%)	τ_2 (ps)	A_3 (%)	τ_3 (ps)
polymer **2**	54 ± 1	1076 ± 73	25 ± 2	54 ± 10	21 ± 2	3 ± 0.7
+20% Zn^{2+}	57 ± 1	1328 ± 41	25 ± 1	213 ± 11	18 ± 2	5 ± 1
+100% Zn^{2+}	56 ± 1	1351 ± 56	15 ± 2	98 ± 30	29 ± 3	10 ± 1
+20% Ni^{2+}	42 ± 2	690 ± 43	31 ± 2	48 ± 8	27 ± 3	4 ± 0.8
+20% Fe^{2+}	24 ± 2	27 ± 3	76 ± 1	3 ± 0.1		

extends to 580 nm. Consequently, only the blue side of the ground-state bleaching region and the red side of the photoinduced absorption region is suitable for obtaining unambiguous kinetics information on the ground-state recovery and excited-state decay. The relative intensities of the photoinduced absorption relative to that of the ground-state bleaching in Zn^{2+}-bound polymer **2** is higher than that in the metal-free polymer when both were excited at 417 nm. This is an indication that the initial excitons are more localized in the Zn^{2+}-bound polymer **2** than in the metal-free polymer, because the photoinduced absorption on the picosecond time scale is largely due to localized excitons.[18,22] Our previous studies on the metal-free polymers show that π-conjugation attenuation promotes localized excitons and longer lifetimes for the photoinduced absorption. The Zn^{2+}-bound polymer **2** has a dominating component of the photoinduced absorption decay with a time constant of 1.3 ns compared to 1.1 ns in the metal-free polymer **2** (Table 1). This confirms that π-conjugation along the polymer chain is attenuated in Zn^{2+}-bound polymer rather than enhanced as we initially expected. More details will be presented later in the Discussion.

The time constants for photoinduced absorption decays at wavelengths >700 nm for metal-ion-incorporated as well as metal-free polymer **2** are listed in Table 1, and the decay curves are displayed in Figure 7. The results indicate that the excited-state decay kinetics for metalated polymer **2** are metal ion specific. For Zn^{2+} (a closed shell metal ion) complexes with polymer **2**, overall excited-state lifetimes are longer than that of the metal-free polymer. However, overall excited-state

TABLE 2: Fluorescence Lifetimes of Metal Ion−Polymer 2 Complexes

compounds	A_1 (%)	τ_1 (ps)	A_2 (%)	$\tau\hat{o}_2$ (ps)	A_3 (%)	τ_3 (ps)
polymer **2**						
probe 520 nm	36 ± 4	940 ± 50	64 ± 4	450 ± 25		
probe 580 nm	36 ± 4	859 ± 50	64 ± 4	462 ± 25		
probe 660 nm	32 ± 4	941 ± 50	68 ± 4	483 ± 25		
+40% Zn^{2+}						
probe @532 nm	41 ± 4	990 ± 50	59 ± 4	464 ± 25		
probe @700 nm	36 ± 4	1750 ± 100	64 ± 4	731 ± 50		
+100% Ni^{2+}						19 ± 10
probe @580 nm	52 ± 4	1740 ± 100	48 ± 4	913 ± 50		
+100% Fe^{3+}	60 ± 4	1905 ± 100	40 ± 4	937 ± 50		125 ± 10
probe @ 466 nm	59 ± 4	1640 ± 100	41 ± 4	728 ± 50		
probe @ 600 nm						

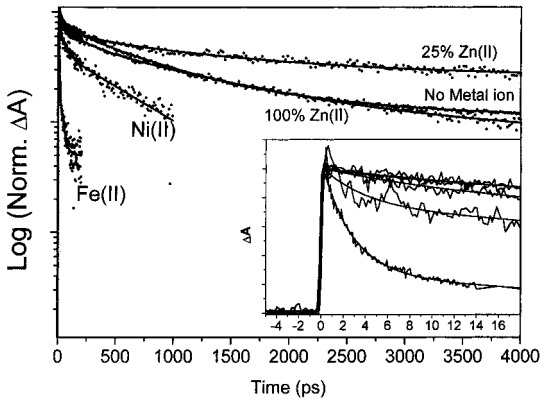

Figure 7. Photoinduced absorption (excited-state absorption) decays of metalated polymer **2**. The inset is an expansion of the early times.

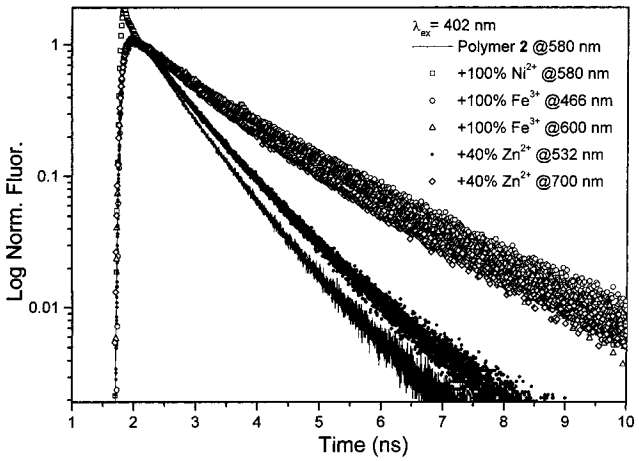

Figure 8. Fluorescence decays of metalated polymers **2** from TCSPC data normalized at long times. Two group curves are shown here with decay times about 0.9 ns for the faster one and 1.6 ns for the slower one.

lifetimes for open shell transition metal ion (such as Ni^{2+} and Fe^{3+}) bound polymers are significantly shorter. The trend in excited lifetimes agrees with excited-state lifetimes of the corresponding simple bpy complexes, where the lifetimes of $[Zn(bpy)_3]^{2+}$ and $[Fe(bpy)_3]^{3+}$ are 1.6 ns and 3 ps, respectively.[23] The correlation between excited-state lifetimes of the simple metal−bpy complexes with the fast components in Table 1 provides evidence that metal ions were bound to the bpy site rather than randomly distributed in the solution.

To obtain the dynamics of the photoluminescent species, fluorescence lifetimes for metal-free polymer **2** and its Zn^{2+}, Ni^{2+}, and Fe^{3+} complexes were measured using TCSPC and are listed in Table 2. Fluorescence lifetimes of the metal-free polymer **2** are nearly the same at different probe wavelengths, with a 1:2 ratio for a 0.8−0.9 ns component to a 0.45 ns component. For polymer **2** with 40% Zn^{2+}-incorporated to the bpy sites, the steady-state PL spectra exhibit two distinguishable fluorescence spectra from metal-free and Zn^{2+}-bound polymer **2**, respectively (Figure 4). Probing at 532 nm, where only fluorescence from the metal-free polymer is present, two decay components similar to those in metal-free polymer **2** were observed. Probing at 700 nm, where very little fluorescence from the metal-free polymer **2** is present, the two fluorescence lifetime components with a 1:2 ratio were 1.75 and 0.73 ns, respectively. For 100% Ni^{2+}-doped polymer **2**, the fluorescence decay has three components with lifetimes of 0.02, 0.91, and 1.74 ns. The shortest component is dominant, and the ratio between the remaining two components is nearly 1:1. Because early work showed a blue shifted fluorescence spectrum in Fe^{3+}-bound polymers, which has a peak at 466 nm, fluorescence decays were collected at two wavelengths at 466 and 600 nm for 100% Fe^{3+}-doped polymer **2** and they appear to have similar time constants. Because of the 50 ps instrument response time in the TCSPC system, some fast fluorescence decay components associated with the 3 ps component in the photoinduced absorption were not detected for Fe^{3+} complex of polymer **2**.

The normalized fluorescence decays of neat and metalated polymer **2** are shown in Figure 8. The fluorescence decay curves are segregated into two groups at longer times. The group with a faster decay is from the metal-free polymer and metal-free segments, and the group with a slower decay is from various metalated polymers **2**. However, with the limited time resolution of the TCSPC system, the fractions for the components with time constants on the short picosecond time scale are likely to be underestimated. Thus, the relative fractions of the two slower components in Fe and Ni-bound polymers are actually smaller.

Structures of Metal Ion Binding Sites in Polymers. Metal ion binding to polymers **1** and **2** significantly changes their photophysical properties. The sources of the changes could come from altering the π-conjugation and introducing charge-transfer states. Using XAFS, the structures around the metal ion binding sites in the polymers can be determined to reveal the sources for the changes in the optical properties. Several specific questions need to be addressed: (1) how metal ions chelate with the bpy groups in the polymer (e.g., monodentate or bidentate); (2) whether metal ions bind to BEH−PPV when there are no bpy binding sites; and (3) if bpy groups from different polymer chains (or other portions of the same polymer chain) bind one metal ion simultaneously. The local structures of metal ion binding sites were compared with those of metal−tris- or bis-bpy complexes. If the polymers bind the metal ions non-specifically, the nearest neighbors of the metal ions would have a broad distribution of the metal-to-atom distances, and the amplitudes for backscattered photoelectron waves from distant neighbors could be distributed over a wide range of distances.

TABLE 3: Metal Ion Binding Site Structures in Polymers

compound	*N*	*R* (Å)	σ^2 (Å^2)
$[Pd^{2+}(bpy)_2](NO_3)_2$	4.0 ± 0.5 (N)	2.03	0.00026
Pd^{2+}−polymer **1**	2.8 ± 0.5 (N)	2.04	0.00436
	4.0 ± 0.5 (O)	2.00	−0.01068
Pd^{2+}−polymer **2**	1.6 ± 0.5 (N)	2.01	−0.00827
	4.6 ± 0.5 (O)	1.98	−0.00367
Pd^{2+}−BEH−PPV	5.1 ± 0.5 (O)	1.99	0.00245
$[Zn(bpy)_3]SO_4$	6.0 ± 0.5 (N)	2.13	0.00002
Zn^{2+}−polymer **1**	2.2 ± 0.5 (N)	2.08 ± 0.02	0.0041
	2.8 ± 0.5 (O)	2.02 ± 0.02	−0.0026
Zn^{2+}−polymer **2**	2.0 ± 0.5 (N)	2.09 ± 0.02	−0.0038
	2.5 ± 0.5 (O)	2.02 ± 0.02	−0.0054
Zn^{2+}−BEH−PPV	4.0 ± 0.5 (O)	2.02 ± 0.02	−0.0020
$[Cu(bpy)_3]SO_4$	2.2 ± 0.5	2.27 ± 0.02	0.008
	4.6 ± 0.5	2.06 ± 0.02	0.003
Cu^{2+}−polymer **1**	2.1 ± 0.5	2.01 ± 0.02	−0.0010
	4.8 ± 0.5	1.97 ± 0.02	0.0096
Cu^{2+}−polymer **2**	2.6 ± 0.5	2.03 ± 0.02	0.010
	4.7 ± 0.5	1.97 ± 0.02	−0.0003
Cu^{2+}−BEH−PPV	1.9 ± 0.5	2.14 ± 0.02	0.0037
	4.2 ± 0.5	1.96 ± 0.02	0.0022
$[Ni(bpy)_3]SO_4$	6.0 ± 0.5	2.09 ± 0.02	0.00004
Ni^{2+}−polymer **1**	2.0 ± 0.5	2.09 ± 0.02	0.003
	4.1 ± 1.0	2.07 ± 0.02	0.001
Ni^{2+}−polymer **2**	2.2 ± 1.0	2.10 ± 0.02	0.004
	4.0 ± 1.0	2.06 ± 0.02	0.001
Ni^{2+}−BEH−PPV	4.4 ± 1.0	2.08 ± 0.02	0.0017

Consequently, the Fourier-transformed XAFS spectra would show a poorly defined, broad peak for the nearest neighbors and nearly invisible peaks for the backscatterings from distant neighbors. If the metal ion binds to the bpy sites with a bidentate configuration, the spectra would show similarities with those of the simple bpy complexes not only in the first coordination shell, but also in the distant neighboring shells, because the rigidity of the bpy group keeps distant atoms well-defined. However, other chelating groups in the polymer may be present simultaneously if only one bpy group is bound. In the case of monodentate binding between the metal ion and the polymer, the relative positions of the atoms other than those from the first shell are less well-defined because of rotation along the metal−N bond. In the third case where one metal ion is bound by more than one bpy group, the structure may not be easily characterized due to the rarity and irregularity of this structure even in a situation with a large excess of the bpy groups relative to the metal ions. Table 3 displays structural parameters for the nearest neighbors of metal ion binding sites in BEH−PPV, polymer **1** and polymer **2**. Figure 9 shows the Fourier-transformed XAFS spectra of metal ion polymer complexes along with the corresponding simple metal−bpy complexes.

The FT-XAFS spectra of Ni^{2+} complexes with polymers **1** and **2** (Figure 9a) show similarities with the corresponding $Ni(bpy)_3$ complex not only on the first shell neighbors but also on the second and the third shell neighbors. The differences are the amplitudes for the distant shells are lower compared to that of the $Ni(bpy)_3$ complex, agreeing with the bidentate binding structure. The data analysis shows that the average Ni−first shell atom distances in the polymer complexes are shorter than those in the $Ni(bpy)_3$ complex and can be best fit into two groups with two N at 2.09−2.10 Å from Ni and four O at 2.06−2.07 Å from Ni. The shorter distances in the polymer complexes are more likely from O atoms from ether groups of the side chains or coordinating methanol, which was used in dissolving the metal salts. Ni^{2+} in BEH−PPV, where no bpy group was present, also shows a well-defined first coordination shell with four O atoms, but its higher shell spectra are different from those of the $Ni(bpy)_3$ complex. This indicates that Ni^{2+} has a tendency of coordinating with either N or O atoms, with a preference to N atoms in bpy groups. The XANES spectrum of the Ni^{2+}−BEH−PPV complex in Figure 10 shows a distinctive shoulder at about 11 eV above the Ni K-edge which implies that Ni^{2+} adopts a square planar geometry in this polymer, whereas this shoulder is missing in the Ni^{2+}−polymer **1** and **2** complexes and in the simple $Ni(bpy)_3$ complex, indicating near octahedral coordination geometries. The Cu^{2+} complexes show the same trend of structural variation as those in Ni^{2+} complexes (not shown).

The Zn^{2+} complexes of the polymers have less pronounced structures in the higher shells compared to other complexes (Figure 9b). However, the average first shell Zn-to-N or O distances in the polymers **1** and **2** complexes are shorter than that in the $Zn(bpy)_3$ complex and longer than that in the Zn−BEH−PPV complex. Because the two-distance fits for the nearest neighbors gave the best results and the similarities between the Zn^{2+} complexes of polymers **1** and **2** and the $Zn(bpy)_3$ in the longer distances region, it is likely the bidentate coordination is present in polymers **1** and **2**.

The Pd^{2+} complexes with BEH−PPV show a well-defined first shell, but no second shell is present (Figure 9c). However, at around 3.4 Å (no phase correction), a peak appears that is likely the second solvation shell of the metal in this polymer matrix. On the other hand, there are well-defined second and third shells for the simple $Pd(bpy)_2$. The complexes with polymers **1** and **2** appear to have spectra that possess a well-defined second shell at $R = 2.2$ Å (uncorrected for phases), slightly less than the second shell in the $Pd(bpy)_2$ complex, but also has higher shell structures between 2.5 and 3.5 Å that resemble those for the Pd−BEH−PPV complex. The average first shell Pd-to-atom distance in polymers **1** and **2** complexes is also smaller than that in the $Pd(bpy)_2$ complex. It is possible that Pd^{2+} chelates with the bpy site of polymers **1** and **2** in a form that is a severely distorted bidentate or monodentate structure, because its second shell, although clearly shown in the spectra, is less than half the amplitude with a shorter distance, as found in the $Pd(bpy)_2$ complex.

For Fe(II)/(III) complexes with polymers **1** and **2** (Figure 9d), a significant increase in the average nearest neighbor distances from that in $Fe^{II/III}(bpy)_3$ complexes was observed, which agrees with the increase of the nearest neighbor distances in Fe(II) complexes when they undergo a spin-state transition from the low spin state to the high spin state. Similar structural changes have been measured before by XAFS.[24] Because bpy is a strong ligand field, Fe(II)/(III) in $Fe(bpy)_3$ has a low spin configuration with a shorter average nearest neighbor distance. However, binding with only one bpy ligand and several much weaker field O ligands in polymers **1** and **2**, Fe(II)/(III) experiences a much smaller splitting of the d orbital energies, resulting in a high spin state with longer nearest neighbor distances. In addition, the Fe(II)/(III) complexes with polymers **1** and **2** have enhanced preedge peaks compared to both the high-spin and low-spin octahedral Fe(II) complexes, indicating the presence of a noncentrosymmetric coordination geometry that is likely distorted octahedral or square pyramidal. The lack of resemblance in the spectra in the longer distance region with that of the high-spin Fe(II) octahedral complex may suggest a possibility of severely distorted bidentate or monodentate binding for Fe in polymers **1** and **2**. It is worth mentioning that the Pd and Fe complexes with the polymers have well-defined second shells but differ significantly from their simple bpy complexes in the longer distance region. Pd and Fe also have smaller binding constants with polymer **2** and require greater than a 1:1 ratio of metal:bpy to reach binding equilibrium, as indicated by the

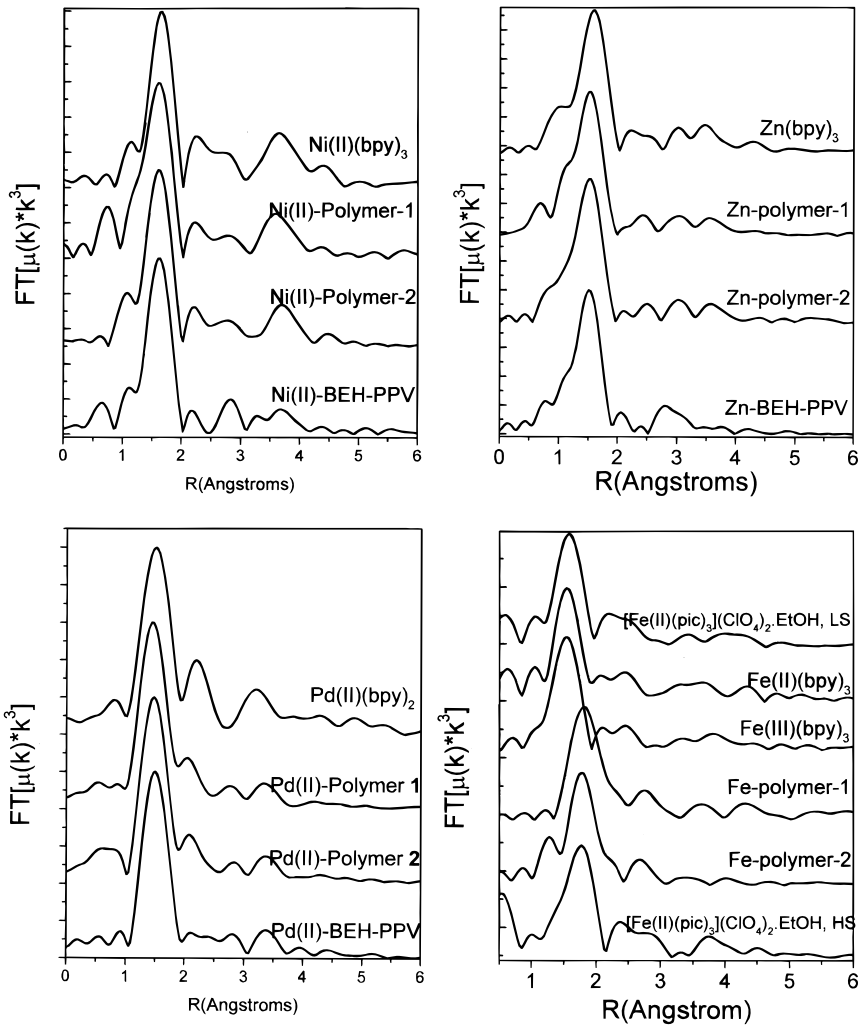

Figure 9. Fourier-transformed XAFS spectra of metalated polymer films (a) Ni^{2+}, (b) Zn^{2+}, (c) Pd^{2+}, and (d) $Fe^{3+/2+}$.

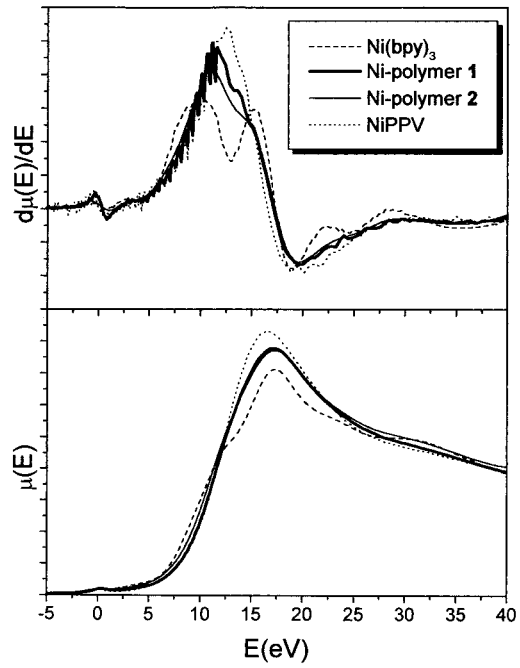

Figure 10. XANES of Ni^{2+}-bound polymers.

titration curves. These observations agree with presence of some monodentate binding of the metal ions, where twice as much of the metal ions is required to saturate all the bpy binding sites.

With all the metal ions studied, there was no obvious difference in the structures of the polymer **1** and **2** complexes. If multiple bpy binding is present, one would expect some difference between the metal ion binding structures between the two complexes, because the relative concentrations of bpy to the polymer chain are different. Complexes of polymers **1** would have a higher probability of forming multiple bpy binding than polymer **2**. However, this is not borne out by the structural measurements.

Discussion

Origins of Red Shifts in Absorption Spectra of Metalated Polymers 1 and 2. As mentioned earlier, metal ion binding to the bpy groups in the polymer chain produces mainly two possible changes to the polymers: (1) restoring planar conformation along the backbone that was segmented by the bpy groups and (2) introducing charge transfer from the metal ion at the bpy sites to the π-conjugated polymer backbone.

The first change was demonstrated by the continuous red shifts of the polymer absorption peak observed in the titration experiments. This type of conformation-induced chromism was also observed in several polythiophene derivatives, where a high-temperature induced a structural disorder caused a blue shift in the absorption spectra.[25] Thus, the origin of the blue shift in the polythiophene is also π-conjugation attenuation due to a nonplanar conformation along the polymer chain. A number of theoretical calculations have demonstrated correlations of

conjugation length in PPV oligomers with their electronic absorption spectra.[26−28] Our previous calculations showed that the lowest electronic transition energies in planar oligomers with the same chemical sequence of polymers **1** and **2** as well as BEH−PPV decrease as the number of π-conjugated bonds increase, and the transition energies for corresponding polymers are in an increasing order as the π-conjugation attenuation, BEH−PPV, polymer **2**, and polymer **1**.[18] Although the lowest electronic transition energies are different, the number of the π-conjugated bonds required for the transition energies to reach plateau or saturation are similar for all three sequences, about seven to eight PV equivalent units.[18]

Because of differences in chemical structure that result from different monomer sequences, the metal ion concentration dependence of the absorption spectra appears to be different between polymers **1** and **2**. For polymer **2**, each metal ion that binds to a bpy group could flatten a section with one bpy group and two adjacent PV trimers, a total of 7.5 PV equivalent units, near the saturation limit of the lowest energy transition. Further binding of a metal ion in an adjacent bpy site may extend the flattened section to 11−12 PV equivalent units, causing little further decrease of the lowest energy transition, or red shift in the absorption peak. Therefore, metal ion titration curves for polymer **2** have well-defined isosbestic points in Figure 3 and can be described by a two-state model, with an unoccupied bpy site P and a metal-ion-occupied site PM in the polymer chain. Whether the metal-ion-occupied bpy site is isolated or adjacent to other occupied sites cannot be distinguished from the titration curves. The binding constants obtained from eq 3 are averaged over all metal binding bpy sites, which assums that there is no interaction between any two sites.

In contrast, poorly defined isosbestic points in metal ion titration curves of polymer **1** suggest that there are more than two binding states during the titration processes. This can be explained also according to our previous calculations on the lowest energy transition as a function of the number of bonds in a π-conjugated system.[18] When a metal ion binds to a bpy site in polymer **1**, it flattens a segment that consists of one bpy−V group and two PV groups, 3.5 PV equivalent units, much shorter than the saturation limit for changes in the lowest electronic transition energy. Additional binding of one and two adjacent bpy sites by metal ions extends the length of the planar segments to six and eight PV equivalent units, respectively, approaching the saturation length for changes in the transition energy. In this case, distinctive absorption spectra could be observed for at least four different species, containing unoccupied, singly, doubly, and triply consecutive bpy sites occupied by metal ions along the polymer **1** chain. Therefore, extracting metal ion binding constants in polymer **1** becomes very difficult. Nevertheless, differences in metal binding titration curves between polymers **1** and **2** provide evidence of the restoration of the planar conformation throughout the polymer chains by the metal binding to the bpy sites.

However, if the metal ion binding to bpy sites merely restores the planar conformation along the backbones in polymers **1** and **2**, the absorption peak positions should have higher energies than that of BEH−PPV based on our ZINDO calculation for planar oligomers representing the three polymers,[18] and all 100% metalated polymers of the same kind should have the same absorption spectra. Clearly this is not the case because ionochromic effects in polymers **1** and **2** have been observed, and the absorption peaks of 100% metalated polymers are at lower energies relative to that of BEH−PPV. For Fe^{2+} and Pd^{2+} complexes with the polymers where either severely distorted bidentate or monodentate binding is likely present, the polymer backbones are not perfectly flattened, but these complexes still give red shifts to lower energies than the BEH−PPV absorption. According to a previous calculation, the lowest energy transitions for polymer **1** and **2** segments always have higher energies than that of BEH−PPV segments with the same number of bonds, when all the segments are planar.[18] This is an indication that the second change that occurs when metal ions bind to the polymers is due to interactions between the polymer backbone and the specific metal ion that occupies the bpy site. That includes the overall influence of the metal ion electrons on the energy gaps of the polymer and from the charge transfer between the metal ion and the bpy groups.

For a π-conjugated polymer backbone, the lowest energy absorption in the visible region is a $\pi-\pi^*$ transition. According to semiempirical quantum mechanical calculations with ZINDO/1, the energy gap between π and π^* shrinks when a π-conjugated segment in the polymer backbone is extended.[18,26−28] Meanwhile, the density of states increases, resulting in a semiconductor-like band structure. When metal ions chelate with the bpy sites in polymers **1** and **2**, the formation of a π overlap between d and p orbitals of the metal ion with the π^* orbitals of the bpy group, i.e., "back-bonding", significantly alters the molecular orbitals and their energy levels of the polymers. The details of such changes have been explored by extensive semiempirical calculations and will be published soon. As a result of the metal incorporation, the energy gaps for $\pi-\pi^*$ transitions, shrink resulting in the red shifts observed in the absorption spectra. Because the electronic structures vary among the metal ions, their influences on the energy levels of the molecular orbitals involving $\pi-\pi^*$ transitions are different. Therefore, ionochromic effects were observed in metal-ion-incorporated polymers **1** and **2** and the energies of the lowest $\pi-\pi^*$ transitions for some metal−polymer complexes are lower than that of a well-conjugated BEH−PPV.

The metal complexes, in which the ligand is part of the polymer, can be considered as metal chelation to a bpy group that is a part of a large π-conjugated system. Compared to a simple bpy ligand, the $\pi-\pi^*$ transition energy is much smaller in polymers **1** and **2**. The energy of the π^* orbital decreases as the π-conjugation is extended. In fact, the lowest $\pi-\pi^*$ transition in polymers **1** and **2** are centered at 438 and 468 nm, compared to that of bpy at 283 nm.[29,30] Therefore, the lowest $\pi-\pi^*$ transitions in polymers **1** and **2** overlap with those from the metal-to-ligand charge-transfer (MLCT) transition of metal−tris-bpy complexes, which are in a spectral range from 440 to 540 nm. Thus, interactions between d and π^* orbitals are stronger in the metal-bound polymers **1** and **2** than in simple bpy complexes. The Stark spectra of several metal−tris-bpy complexes from a previous study reveal that the coupling between the $\pi-\pi^*$ and MLCT transitions increase as the energies of these two transitions get closer.[31] Moreover, other studies indicate that the MLCT transition energies are lowered in Ru−bpy complexes when one of the bpy ligands has extended π-conjugation, resulting in red shifts in the absorption and the emission spectra as well as an increase in the excited-state lifetime.[31,32] Therefore, the red shifts observed in metal-ion-bound polymers **1** and **2** are due to both alternations in $\pi-\pi^*$ transition energy gaps as well as conformation flattening. The coexistence of the $\pi-\pi^*$ transition and the MLCT transition in metal-ion-incorporated polymers **1** and **2** gives their dual photophysical behaviors as a π-conjugated photoconducting polymer and as a metal−bpy complex.

Exciton Dynamics and Dual Photophysical Behavior of Metalated Polymers 1 and 2. The dual properties of metal-ion-incorporated polymers **1** and **2**, as conjugated polymers and as metal complexes, can be used to explain the observed exciton dynamics in these polymers. The photoluminescence and excited-state absorption decay kinetics of metalated polymer **2** are dominated by its behavior as a bpy complex. Different behaviors of PL for Zn- and Ni-bound polymer **2** are first examined. Zn^{2+} has a d^{10}, closed shell electronic configuration and it cannot be further oxidized. Therefore, the only possible transition in Zn^{2+}-polymer complexes is an intraligand $\pi-\pi^*$ transition or ligand-to-ligand charge-transfer (LLCT) transition.[33] Thus, in Zn^{2+}-bound polymer **2**, the red-shifted photoluminescence occurs from the π^* state as a result of Zn^{2+} chelation to the conjugated polymer backbone. In other words, the π orbitals of polymer **2** are changed due to the influence from the electrons in Zn^{2+}, as mentioned above. Because the π-conjugation along the backbone is attenuated by the bpy sites in metal-free sections of polymer **2**, the nonplanar conformation along the chain separates Zn^{2+}-occupied and unoccupied segments. Thus, both red-shifted and unshifted $\pi-\pi^*$ transitions occur simultaneously in partially occupied Zn^{2+} polymer **2**. Since both transitions result in photoluminescence, we observed dual peaks in the emission spectra. In contrast, Ni^{2+} has a d^8 electronic configuration and is more stable as a triplet in the ground state, so its MLCT transition is not a singlet state due to strong spin−orbit coupling between the metal and the ligands. This leads to fluorescence quenching and an increase in nonradiative decay rate. However, because of weak interactions between metal-occupied and unoccupied segments along the polymer chain, fluorescence quenching by Ni^{2+} binding does not influence the entire polymer and PL from unoccupied segments due to $\pi-\pi^*$ transitions is virtually unchanged. In other words, because the electronic overlap between the metal-occupied and unoccupied segments is small, energy transfer is not efficient along the chain, which prevents the PL from the unoccupied section from being quenched.

Similarly, the differences in the excited-state absorption decay kinetics monitored above 700 nm among metalated polymers can be related to their behavior as bpy complexes. With the same arguments about the electronic configuration of d orbitals as above, Ni^{2+} and Fe^{3+} complexes with polymer **2** have very short excited-state lifetimes due to their open shell d electron configuration and hence large spin−orbit couplings. Zn^{2+}-bound polymer **2**, on the other hand, does not have the same nonradiative decay routes as Ni^{2+} and Fe^{3+} polymers, so its exciton lifetime of 1.3 ns is longer than the 1.0 ns observed for the metal-free polymer **2.** The Zn^{2+} polymer **2** complex demonstrates the influence of metal electron participation in π-conjugation without spin−orbit coupling and MLCT transition. Also indicated in Figure 6, the Zn^{2+}-bound polymer **2** has a higher photoinduced absorption intensity compared to that of the metal-free polymer, implying that the conjugation lengths or interactions between different segments along the polymer backbone are smaller in the Zn^{2+}-bound polymer. This conclusion agrees with the observed longer lifetimes for photoluminescence and photoinduced absorption changes in Zn^{2+}-bound polymer **2.** Although the backbone of polymer **2** may be flattened and extended by Zn^{2+} binding, the differences in electronic structures of metal-ion-occupied bpy site and the adjacent PV units generate high energy barriers for the exciton to travel along the polymer chain. This agrees with our earlier observation of increasing lifetimes of the photoluminescence and photoinduced absorption in metal-free polymers on the order of BEH−PPV, polymer **2**, polymer **1**, where π-conjugation is increasingly attenuated.[18]

The two groups of PL decays on a long time scale for metal-ion-free and metalated polymer **2** shown in Figure 8 can be explained by their properties as a π-conjugated polymer. The metal ion dependent decays in the short time scale are due to their MLCT transitions, whereas the decay rate constants for the longest components are virtually metal independent and are due to $\pi-\pi^*$ transitions of the polymer under the condition of metal ion participation of the π bonding. Suppose there is a series of variations of the polymers where the number of the PV units between the bpy groups could vary from one to many. The question is: what is the limit when the photophysical behavior of the polymer is taken over by that of the metal complexes? When the excitation photon energy exceeds the transition energies of both $\pi-\pi^*$ and MLCT transitions, both processes could occur and the branching ratio from the π^* state to radiative and to nonradiative decay pathways determines the optical properties of the polymer. The metal independent PL observed in the TCSPC measurements for metal-bound polymers is the remaining portion of the radiative decay originating from the π^* state. When the MLCT transition is absent, like in the Zn^{2+} case, the PL from the π^* state is strong; when the MLCT transition is present, like in Ni^{2+} and Fe^{3+} cases, the majority of the π^*-state population undergoes nonradiative decay via spin−orbit coupling, while a very small fraction of the π^*-state population still emits metal ion independent PL.

In our previous studies on conjugated polymer solutions without metal ions, the electronic coupling between monomer units along the chain was considered crucial to the photophysical properties of the polymers. This concept is also applicable to metalated polymers, only the situation becomes more complex. On one hand, metal ion binding restores the planar conformation along the chain, which favors stronger interactions between the segments, therefore, stronger π-conjugation. On the other hand, the differences between electronic structures of a metal-ion-occupied bpy unit and that of a BEH−PV unit are more significant than that between a bpy unit and a BEH−PV unit, providing unfavorable interactions between the segments along the polymer chain. Such structural incompatibility results in quantum confinement of excitons along the polymer chain even in a planar conformation. Previous studies on the metal-free polymers indicate that the excited-state lifetimes are in the order BEH−PPV < polymer **2** < polymer **1**, because of increasing quantum confinement. Thus, when the spin−orbit coupling of the metal ion with the polymer ligand is absent, the longer component of the excited-state lifetimes in the metalated polymers are likely due to the same reason. However, the quantum confinement in metal-free polymers is mainly due to nonplanar conformations, whereas that in metalated polymers results from electronic structural incompatibilities between the metalated bpy with adjacent PV units.

Summary

Photophysical properties of metalated polymers **1** and **2** can be described by their dual properties as metal-chelated conjugated polymers and as bpy complexes. The participation of the electrons from the metal ions in the π-conjugation of the polymers alters energy gaps for the $\pi-\pi^*$ transition, resulting in ionochromic effects absorption and photoluminescence. Although metal ion binding to the bpy groups in the backbone of the polymers restores planar conformation, it also introduces potential barriers along the backbone due to incompatibility between the electronic structures of the metal complexes and

the PV units, causing quantum confinement of excitons. The photoluminescence and excited-state absorption spectra of the metal ion polymers are largely dependent on the metal ions. Closed shell metal ion complexes of polymers **1** and **2** have longer excited-state lifetimes and higher photoluminescence quantum yields compared to the metal-free polymers, whereas open shell metal ion complexes have very short excited-state lifetimes and their photoluminescence is largely quenched due to nonradiative decay of the excitons via strong spin−orbit couplings. From the point of view of photonic applications, the closed shell metal ion binding to polymer **2** could be used to shift absorption and emission spectra and to enhance photoluminescence quantum efficiency, whereas the open shell metal complexes could be used in metal ion sensing.

Acknowledgment. This work was supported by the Environmental Management Science Program (W.J.H.J., M.P.N., D.J.G.) and by the Division of Chemical Sciences, Office of Basic Energy Sciences (L.X.C., W.J.H.J., M.R.W.), U.S. Department of Energy under contract W-31-109-Eng-38. The authors would like to thank Professor Russell H. Schmehl and Dr. Eric S. Manas for their helpful discussions and comments.

References and Notes

(1) Burroughes, J. H.; Bradkey, D. D.; Brown, A. R.; Marks, R. N.; Mackay, K.; Friend, R. H.; Burn, P. L.; Holmes, A. B. *Nature* **1990**, *347*, 539.

(2) For a recent review, see: Leising, G.; Tasch, S.; Graupner, W. In *Handbook of Conducting Polymers*; Skotheim, T. A., Elsenbaumer, R. L., Reynolde, J. R., Eds.; M. Dekker: New York, 1998; p 847.

(3) Friend, R. H.; Greenham, N. C. In *Handbook of Conducting Polymers*; Skotheim, T. A., Elsenbaumer, R. L., Reynolde, J. R., Eds.; M. Dekker: New York, 1998; p 823.

(4) Friend, R. H.; Denton, G. J.; Halls, J. J. M.; Harrison, N. T.; Holmes, A. B.; Köhler, Lux, A.; Moratti, S. C.; Picher, K.; Tessler, N.; Towns, K.; Wittmann, H. F. *Solid State Commun.* **1997**, *102*, 249.

(5) Tessler, N.; Denton, G. J.; Friend, R. H. *Nature* **1996**, *382*, 695.

(6) Hide, F.; Diaz-Garcia, M. A.; Schwartz, B. J.; Anderson, M. R.; Fei, Q.; Heeger, A. J. *Science* **1996** *273*, 1833.

(7) Frolov, S. V.; Gellermann, W.; Ozak, M.; Yoshino, K.; Vardeny, Z. V. *Phys. Rev. Lett.* **1997** *78*, 729.

(8) Peng, Z.; Gharavi, A. R.; Yu, L. *J. Am. Chem. Soc.* **1997**, *119*, 4622.

(9) Wang, B.; Wasielewski, M. R. *J. Am. Chem. Soc.* **1997**, *119*, 12.

(10) Ley, K. D.; Whittle, E.; Bartberger, M. D.; Schanze, K. S. *J. Am. Chem. Soc.* **1997**, *119*, 3423.

(11) Kimura, M.; Horai, T.; Hanabusa, K.; Shirai, H. *Adv. Mater*. **1998**, *10*, 459.

(12) Davis, W. B.; Svec, W. A.; Ratner, M. A.; Wasielewski, M. R. *Nature* **1998**, *365*, 60.

(13) Jiang, H.; Yang, S.-W.; Jones, W. E., Jr. *Chem. Mater.* **1997**, *9*, 2031.

(14) Schlicke, B.; Belser, P.; De Cola, L.; Sabbioni, E.; Balzani, V. *J. Am. Chem. Soc.* **1999**, *121*, 4207.

(15) Rassmussen, S. C.; Thompson, D. W.; Singh, V.; Peterson, J. D. *Inorg. Chem.* **1996**, *35*, 3449.

(16) Yamamoto, T.; Maruyama, T.; Zhou, Z.; Ito, T.; Fukuda, T.; Yoneda, Y.; Begum, F.; Ikeda, T.; Sasaki, S.; Takezoe, H.; Fukuda, A.; Kubota, K. *J. Am. Chem. Soc.* **1994**, *116*, 4832.

(17) Yamamoto, T.; Yoneda, Y.; Maruyama, T. *J. Chem. Soc. Commun.* **1992**, 1652.

(18) Chen, L. X.; Jäger, W. H. G.; Niemcyzk, M. P.; Wasielewski, M. R. *J. Phys. Chem. A* **1999**, *103*, 4341.

(19) (a) Bray, R. G.; Ferguson, J.; Hawkins, C. J. *Aust. J. Chem.* **1969**, *22*, 2091. (b) Ferguson, J.; Hawkins, C. J.; Kane-Maguire, N. A. P.; Lip, H. *Inorg. Chem.* **1969**, *8*, 771.

(20) O'Connor, D. V.; Phillips, D. *Time-correlated Single Photon Counting,;* Academic Press: London, 1984.

(21) Greenfield, S. R.; Svec, W. A.; Gosztola, D.; Wasielewski, M. R. *J. Am. Chem. Soc*. **1996**, *118*, 6767.

(22) (a) Yan, M.; Rothberg, L. J.; Papadimitrakopoulos, F.; Galvin, M. E.; Miller, T. M. *Phys. Rev. Lett.* **1994**, *72*, 1104. (b). Hsu, J. W. P.; Yan, M.; Jedju, T. M.; Rothberg, L. J. *Phys. Rev. B* **1994**, *49*, 712.

(23) Kalyanasundaram, K. *Photochemistry of Polypyridine and Porphyrin Complexes*; Academic Press: London, 1992; p 93.

(24) Chen, L. X.; Wang, Z.; Burdett, J. K.; Montano, P. A.; Norris, J. R. *J. Phys. Chem*. **1995**, *99*, 7958.

(25) Leclerc, M.; Faïd, K. In *Handbook of Conducting Polymers*; Skotheim, T. A., Elsenbaumer, R. L., Reynolde, J. R., Eds.; M. Dekker: New York, 1998; p 695.

(26) Beljonne, D.; Cornil, J.; dos Santos, D. A.; Shuai, Z.; Bredas, J. L. In *Primary Photoexcitations in Conjugated Polymers: Molecular Exciton versus Semiconductor Band Model*; Sariciftci, N. S., Ed.; World Scientific: Singapore, 1998; Chapter 19.

(27) Janssen, R. A. J. In *Primary Photoexcitations in Conjugated Polymers: Molecular Exciton versus Semiconductor Band Model*; Sariciftci, N. S., Ed.; World Scientific: Singapore, 1998; Chapter 18.

(28) Bredas, J. L.; Cornil, J.; Meyers, F.; Beljonne, D. In *Handbook of Conducting Polymers*; Skotheim, T. A., Elsenbaumer, R. L., Reynolde, J. R., Eds.; M. Dekker: New York, 1998; p 1.

(29) Bandyopadhyay, B. A.; Harriman, A. *J. Chem. Soc., Faraday Trans. 1* **1977**, *73*, 663.

(30) Harriman, A. *J. Photochem.* **1978**, *8*, 618.

(31) Hug, S.; Boxer, S. G. *Inorg. Chim. Acta* **1996**, *242*, 323.

(32) Strouse, G. F.; Schoonover, J. R.; Duesing, R.; Boyde, S.; Jones, W. E., Jr.; Meyer, T. J. *Inorg. Chem.* **1995**, *34*, 473.

(33) Shaw, J. R.; Webb, R. T.; Schmehl, R. H. *J. Am. Chem. Soc*. **1990**, *112*, 1117.

(34) Kutal, C. *Coord. Chem. Rev.* **1990**, *99*, 213.